Autonomous Active and Reactive Power Distribution Strategy in Islanded Microgrids

Wu, Dan; Tang, Fen; Guerrero, Josep M.; Vasquez, Juan Carlos; Chen, Guoliang; Sun, Libing

Published in:
Proceedings of the 29th Annual IEEE Applied Power Electronics Conference and Exposition, APEC 2014

DOI (link to publication from Publisher):
10.1109/APEC.2014.6803600

Publication date:
2014

Document Version
Early version, also known as pre-print

This document is a pre-print of the final paper:
D. Wu, F. Tang, J. M. Guerrero, J. C. Vasquez, G. Chen, L. Sun, "Autonomous active and reactive power distribution strategy in islanded microgrids," IEEE Applied Power Electronics Conference and Exposition, IEEE APEC 2014.

Autonomous Active and Reactive Power Distribution Strategy in Islanded Microgrids

Dan Wu[1], Fen Tang[2], Josep M. Guerrero[1], Juan C. Vasquez[1]
[1] Department of Energy Technology, Aalborg University, Denmark
[2] School of Electrical Engineering, Beijing Jiaotong University, P. R. China
{dwu, joz, juq}@et.aau.dk, ftang_nego@126.com

Guoliang Chen, and Libing Sun
Technology Center
Shanghai Solar Energy & Technology Co., Ltd.
Shanghai, P. R. China
{chengl1968, slb-job}@163.com

***Abstract*— This paper proposes an autonomous active and reactive power distribution strategy that can be applied directly on current control mode (CCM) inverters, being compatible as well with conventional droop-controlled voltage control mode (VCM) converters. In a microgrid, since renewable energy sources (RES) units regulate different active power, the proposed reactive power distribution is adaptively controlled according to the active power distribution among energy storage systems (ESS) and RES units. The virtual impedance is implemented in order to improve the reactive power sharing in a distributed way. Real-time hardware-in-the-loop results are presented to verify the proposed control strategy.**

I. INTRODUCTION

Microgrids are providing a promising way to integrate distributed generators (DG) such as renewable energy sources (RES) and energy storage systems (ESS) to supply power to local loads [1]. Among the control strategies investigated in islanded microgrids, master-slave control structure is the most popular way to manage the ESS and RES units, where the ESS units operate as grid forming units and RES units operate as grid following units [2].

Usually, RES units control output active power by using maximum power point tracking strategies, and deliver no reactive power. Therefore almost all of the reactive power from demand side is provided by the ESS units. However, considering the total output power rating of the converter is fixed, the more reactive power delivered from ESS units, the less capacity of active power regulation of ESS used to buffer the unbalance of power generation and consumption can be provided. In order to overcome such a limitation, many previous researches have been carried out to investigate the implementation that using RES units to provide reactive power support and improve power quality [3], [4]. However, these methods are based on setting fixed reactive power commands of RES units intensively. And the proportional active and reactive power sharing should be fulfilled by using a microgrid central controller to adjust the power references of RES units with additional communication link [5].

Alternatively, in order to achieve the power sharing in a fully decentralized way, droop method can be a good solution for the voltage controlled mode (VCM) converters [6], [7]. A frequency-bus-signaling control for the power management based on droop control is proposed in [8], and a coordinated control for the active power distribution among ESS and RES units is proposed in [9]. However, the conventional reactive power-to-voltage (Q–V) droop method is mostly used on VCM inverters, which is difficult to be applied directly on RES inverters since they are often current controlled mode (CCM) inverters with only current inner loop. In this sense, this paper presents a voltage-to-reactive power (V–Q) reverse droop control strategy that can be applied on CCM inverters to allow VCM/CCM units coordination when sharing the demanded reactive power. In order to ensure proper autonomous power sharing based on basic droop and reverse droop method, this paper proposes an advanced primary control that taking into account of the system capacity. Furthermore, since the voltage drop over the line impedance will create inaccuracy of reactive power distribution, this phenomenon is also discussed in this paper.

This paper is organized as follows. The principle of the basic primary control, and advanced primary control taking into account of the system capacity are illustrated in the Section II. Section III provides the analysis for the accuracy of reactive power sharing and the corresponding solutions for the improvement. Section IV describes the system control implementation. The real-time hardware-in-the-loop results are presented in Section V. Finally Section VI gives the conclusion.

II. PRIMARY CONTROL FOR VCM AND CCM

A. Droop and Reverse Droop Control

An islanded microgrid with both VCM and CCM units is shown in Fig. 1. In order to achieve autonomous active/reactive power sharing among DG units operating in VCM, droop control is often used in primary loop (considering output impedance is inductive) [6]

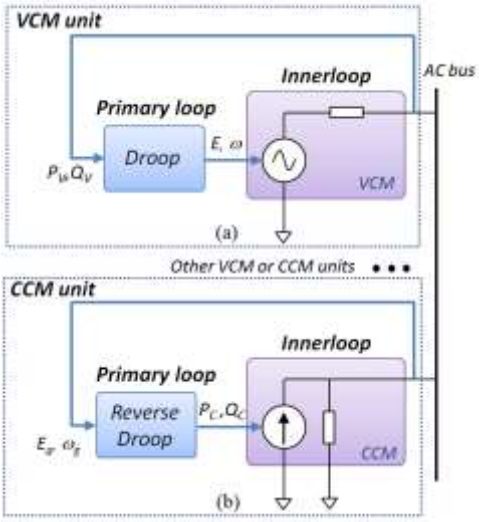

Fig. 1. System configuration of VCM (a) and CCM (b).

$$\omega = \omega^* - m_d P_V \tag{1}$$

$$E = E^* - n_d Q_V \tag{2}$$

where ω and E are the output frequency and voltage of converters, ω^* and E^* are their nominal values respectively, P_V and Q_V are the output active and reactive power of VCM converters, m_d and n_d are the droop coefficients. The droop control characteristic of active/reactive power regulation is shown in Fig. 2.

For the DG units operating in CCM, the active and reactive power is regulated directly by inner current loop. In order to contribute to regulate the AC bus frequency/amplitude, reverse droop can be applied as,

$$P_C = \frac{1}{m_r}(\omega^* - \omega_g) \tag{3}$$

$$Q_C = \frac{1}{n_r}(E^* - E_g) \tag{4}$$

where ω_g and E_g are the measured grid frequency and voltage of CCM units, P_C and Q_C are the output active and reactive power of CCM converters, m_r and n_r are the droop coefficients. The reverse droop control characteristic of frequency/voltage regulation is shown in Fig. 3.

Supposing $E=E_g$ and $\omega=\omega_g$ in ideal case of measurement, and ignoring the inner-loop regulation with higher bandwidth, we have the power distribution of the DG system integrating both VCM and CCM units by combing (1)-(4),

$$P_1 : P_2 \cdots : P_i = \frac{1}{m_1} : \frac{1}{m_2} \cdots : \frac{1}{m_i} \tag{5}$$

$$Q_1 : Q_2 \cdots : Q_i = \frac{1}{n_1} : \frac{1}{n_2} \cdots : \frac{1}{n_i} \tag{6}$$

where P_i and Q_i are the output active and reactive power of each unit, m_i and n_i are the droop/reverse droop coefficients of active and reactive power respectively. According to (5) and (6), the active/reactive power distribution can be simply achieved by assigning proper sets of coefficients of m_i and n_i in a distributed way.

B. *Primary Control Considering System Capacity and Power Availability*

In practical cases, the active/reactive power distribution should take into consideration of power availability of RES operating in CCM, and capacity constraint of each system. In this sense, the active power regulation for VCM and CCM should meet the demand of (i) the active power of CCM operates at maximum power point (MPP) and (ii) the VCM units share the remained active power according to the capacity. Therefore, the active power command of CCM shown in (3) is changed as

$$P_C = P^* \tag{7}$$

where P^* denotes the generated maximum power reference based on the energy sources condition. And the droop coefficient of VCM is designed as

$$0 < m_d \le \frac{\Delta\omega}{P_{\max V}} \tag{8}$$

where P_{maxV} and $\Delta\omega$ are maximum output active power and corresponding bus frequency deviation respectively.

In terms of the reactive power regulation, the maximum available reactive power of each unit is expressed as

$$Q_{\max} = \sqrt{S_{\max}^{\ 2} - P^2} \tag{9}$$

where $Q_{\max}$ and $S_{\max}$ are the maximum reactive power and apparent power of each unit, P is instantaneous power. It is

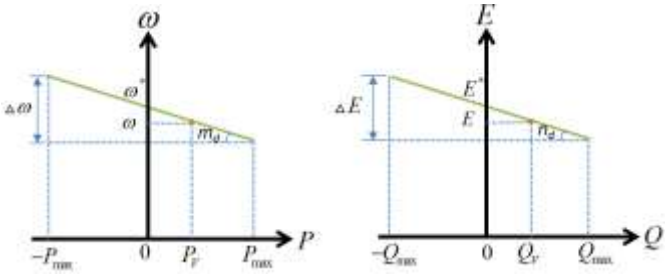

Fig. 2. Droop characteristic of active/reactive power regulation.

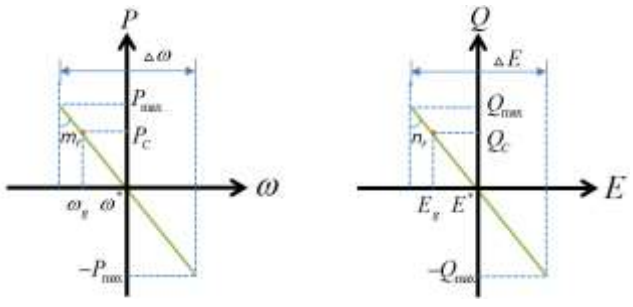

Fig. 3. Reverse droop characteristic of frequency/voltage regulation.

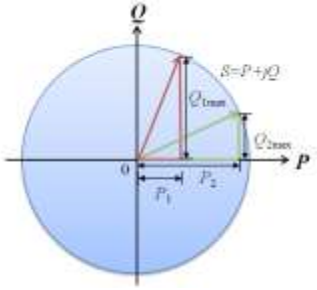

Fig. 4. Relationship of power regulation of two units.

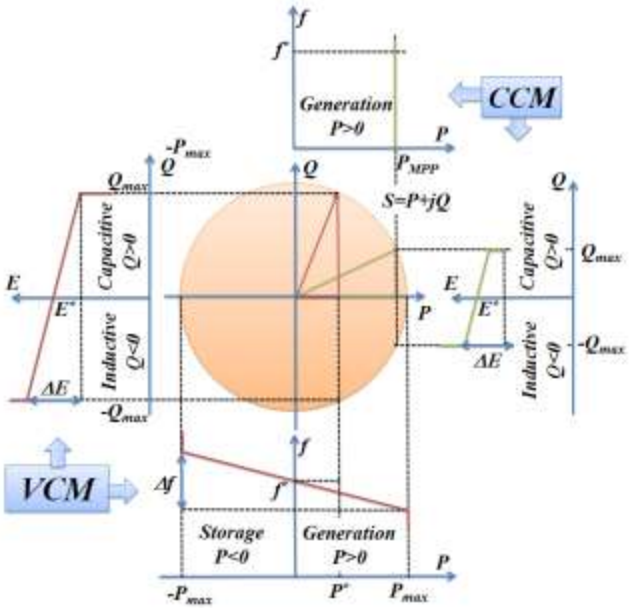

Fig. 5. Active power and reactive power distribution for VCM and CCM units.

shown that the reactive power availability is not only related to the power rating of the unit but also the instant output active power. The relationship of power regulation of two units is shown in Fig. 4, which shows that the more active power the unit supplies, the less capacity of reactive power regulation is remained under the same total apparent power.

Therefore, instead of independently controlling the reactive power with constant coefficient n_d and n_r for (2) and (4), autonomous reactive power control can be achieved with adaptively adjusting the droop/reverse droop coefficients n as

$$n = \frac{\Delta E}{\sqrt{S_{\max}{}^2 - P^2}} \tag{10}$$

where ΔE is maximum bus voltage amplitude deviation, n is droop/reverse droop coeffecient. Both frequency and voltage amplitude deviation in (8) and (10) should be designed within the requirement of grid code. Then, based on (10), the reactive power distribution among integrated VCM and CCM units can be deduced as

$$Q_1 : Q_2 \cdots : Q_i = \sqrt{S_{\max}{}^2 - P_1^2} : \sqrt{S_{\max}{}^2 - P_2^2} \cdots : \sqrt{S_{\max}{}^2 - P_i^2} \tag{11}$$

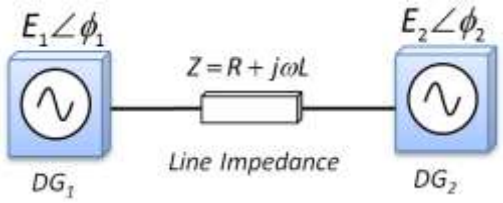

Fig. 6. Equivalent circuit of two DG units connected by line impedance.

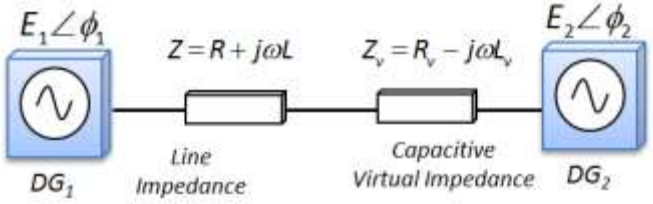

Fig. 7. Principle of reactive power compensation using virtual impedance.

Fig. 5 shows the active power and reactive power distribution for VCM and CCM units. For VCM units, both active and reactive power is based on droop control, and for CCM units, the active power is based on MPP regulation, and reactive power is based on reverse droop control. The active /reactive power control of both VCM and CCM units should be constrained by the total apparent power which is represented as the circle in Fig. 5.

III. Improvement on Reactive Power Sharing

In islanded microgrid, all the DG units share the same frequency signal so that the active power can be well distributed based on droop control. However the voltage drop over the line impedance can be different among DG units so that the reactive power is hard to achieve accurate distribution. Fig. 6 shows the equivalent circuit of two DG units connected by line impedance.

According to (2) and (4), the reactive power difference between DG_1 and DG_2 can be expressed as

$$Q_{dif} = \frac{E_2^* - E_2}{n_2} - \frac{E_1^* - E_1}{n_1} \tag{12}$$

where n_1 and n_2 are defined as (10). Supposing the two DG units have the same reactive power capacity, then we have $n_1=n_2=n$, (12) can be deduced as

$$Q_{dif} = \frac{\left[(E_2^* - E_1^*) - (E_2 - E_1)\right]}{n} = \frac{(E_{dif}^* - E_{dif}) \cdot Q_{\max}}{\Delta E} \tag{13}$$

where E_{dif} is the voltage drop on the line impedance, and $E_{dif}^* = E_2^* - E_1^*$. It shows that the suppression of reactive power difference can be obtained by increasing ΔE. In this case, the performance of Q_{dif} deduction is constrained by the maximum voltage amplitude deviation (i.e. 10% of nominal voltage deviation according to EN 50160) and the output voltage regulation is thereby deteriorated. In the other case, the reduction of Q_{dif} can be achieved by decreasing $E_{dif}^* - E_{dif}$. Since E_{dif} is generated by the line impedance, a secondary

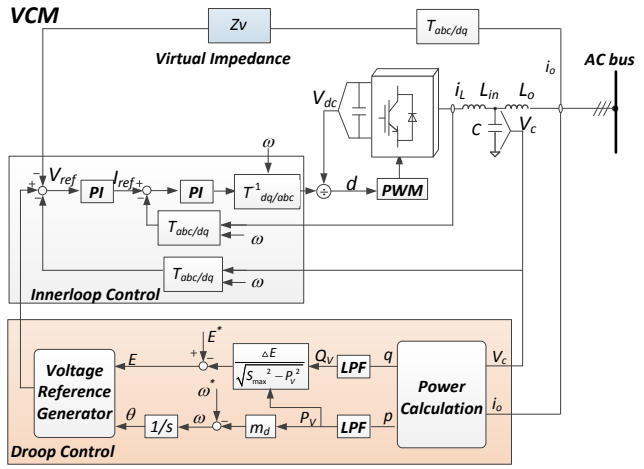

(a)

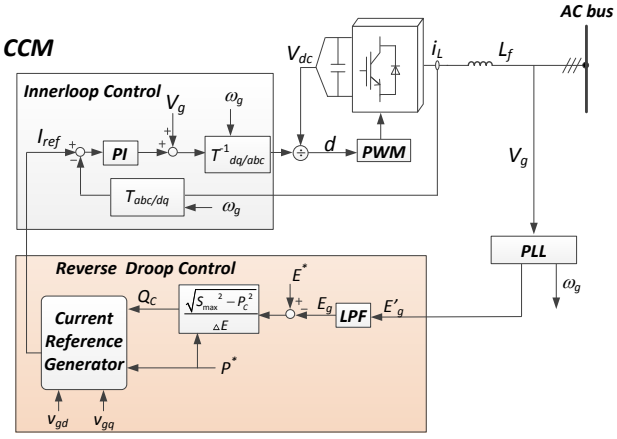

(b)

Fig. 8. Control Algorithms of VCM and CCM

control can be utilized to compensation E_{dif} by adjustment of E_{dif}^* with communication [10] or using virtual impedance to compensate the voltage drop in a distributed way [11].

The principle of reactive power compensation using virtual impedance is shown in Fig. 7. Since the reactive power difference of DG units is produced by the line impedance, the idea of virtual impedance is adding Z_v on the reference in the control loop to compensate the voltage drop. Supposing the line impedance is inductive, and then the virtual impedance can be designed as capacitive for the compensation. To improve the system damping, a positive virtual resistance can be added on the system. Therefore, the compensating voltage reference of DG units can be expressed as

$$\vec{V}_{co} = \vec{I}_o \cdot Z_v = \vec{I}_o \cdot (R_v - j\omega L_v) \tag{14}$$

where L_v and R_v are the virtual inductance and resistance, $\vec{V}_{co}$ and $\vec{I}_o$ are the vector of compensating voltage reference and output current.

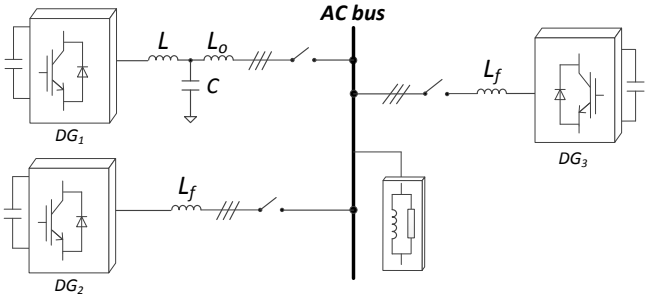

Fig. 9. System configuration of hardware-in-the-loop simulation.

IV. CONTROL IMPLEMENTATION

The control implementation of DG units controlled in VCM and CCM is shown in Fig. 8, which consists of inner-loop control, primary control and virtual impedance.

A. Inner-loop

The inner-loop control of VCM and CCM targets at good tracking performance of output voltages and currents respectively. For both VCM and CCM units, typical proportional integral (PI) controller is used with reference frame transformation $T_{abc/dq}$ and $T^{-1}_{dq/abc}$ between *d-q* and *abc* reference frame. The design procedure of inner-loop control can be referred to [12]. Compared to the classical independent inner-loop control, it worth noticing that the frequency signal used in the reference frame transformation for VCM is generated from primary droop control.

B. Primary Loop

For primary loop of VCM units, droop control based on (1), (2) and (10) is used. While for CCM units, reverse droop based on (3), (4) and (10) is used. When the active power of the converter reaches the maximum value S_{max}, the output reactive power should be limited to zero. The low pass filter (LPF) used in the primary control aims at limiting the loop bandwidth, so that the primary control can be separately designed and the innerloop of VCM and CCM can be considered as ideal voltage and current source respectively. The voltage reference generator of VCM is presented as

$$v_{refd} = E \cdot \cos\theta \tag{15}$$

$$v_{refq} = E \cdot \sin\theta \tag{16}$$

where v_{refd} and v_{refq} are the voltage references sent to the innerloop, θ is the phase angle. And the current reference generator block is expressed as

$$i_{refd} = \frac{2}{3}\left(\frac{v_{gd}}{E_g} \cdot P_C + \frac{v_{gq}}{E_g} \cdot Q_C\right) \tag{17}$$

$$i_{refq} = \frac{2}{3}\left(\frac{v_{gq}}{E_g} \cdot P_C - \frac{v_{gd}}{E_g} \cdot Q_C\right) \tag{18}$$

where i_{refd} and i_{refq} are the current references sent to the innerloop.

TABLE I. POWER STAGE AND CONTROLLER PARAMETERS

Parameter	Symbol	Value	Unit
Power Stage			
Nominal Bus Voltage	V^*	220	V
Nominal Bus Frequency	f^*	50	Hz
Filter Inductance of DG_1	L	1.8	mH
Filter Inductance of DG_2 and DG_3	L_f	3.6	mH
Filter Capacitance	C	9	μF
Line Inductance	L_o	1.8	mH
Line Resistance	r_o	0.1	Ω
Load	R,L	96.8, 0.38	Ω/H
Innerloop Control			
Voltage Loop PI	k_{pV}, k_{iV}	0.1, 200	-, s^{-1}
Current Loop PI	k_{pI}, k_{iI}	15, 50	-, s^{-1}
Primary Control/Virtual Vmpedance			
Frequency Droop	m_d	0.0005	rad·s^{-1}/W
Voltage Droop	n_d	0.0013, 0.0053	V/Var
Frequency Reverse Droop	m_r	0.0005	rad·s^{-1}/W
Voltage Reverse Droop	n_r	0.0013, 0.0053	V/Var
Capacitive Virtual Impedance	$-L_v$	-1.75	mH

C. *Virtual Impedance*

Capacitive virtual impedance is utilized to compensate the reactive power difference. The virtual impedance should be designed near to the value of line impedance to cancel the voltage drop. For *d-q* reference frame control system, (14) is rewritten as

$$v_{cod} = R_v \cdot i_{od} + \omega L_v \cdot i_{oq} \tag{19}$$

$$v_{coq} = R_v \cdot i_{oq} - \omega L_v \cdot i_{od} \tag{20}$$

where v_{cod}, v_{coq} and i_{od}, i_{oq} represent the *d-q* components of compensating voltages and output currents. Then the compensating voltage is added to the voltage reference in the innerloop to decrease E_{dif}.

V. HARDWARE-IN-THE-LOOP RESULTS

Hardware-in-the-loop simulations are carried out based on dspace1006 platform to validate autonomous active and reactive power distribution control strategy for VCM and CCM units. The system configuration is shown in Fig. 9, where the DG_1 operates in VCM with droop control, and DG_2 and DG_3 operate in CCM with reverse droop. The power stage and control system parameters are shown in Table I.

Fig. 10 shows the simulation results of active and reactive power distribution with the variation of droop/reverse droop coefficients. For DG_1, droop control is applied on both active and reactive power, while for DG_2 reverse droop is only applied on reactive power and active power control utilizes a constant power tracking at 1kW. In order to evaluate the reactive power sharing accuracy, the droop/reverse droop coefficients is selected the same as n_d=n_r=0.0013. DG_2 starts up at t_1, and supply active and reactive power to the grid automatically. It can be seen reactive power difference Q_{dif} is

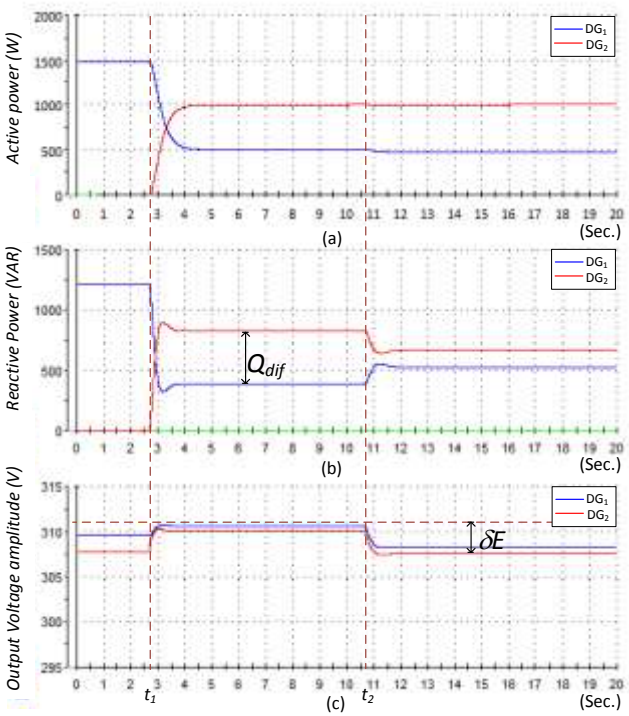

Fig. 10. Active and reactive power distribution with droop/reverse droop coefficients changes.

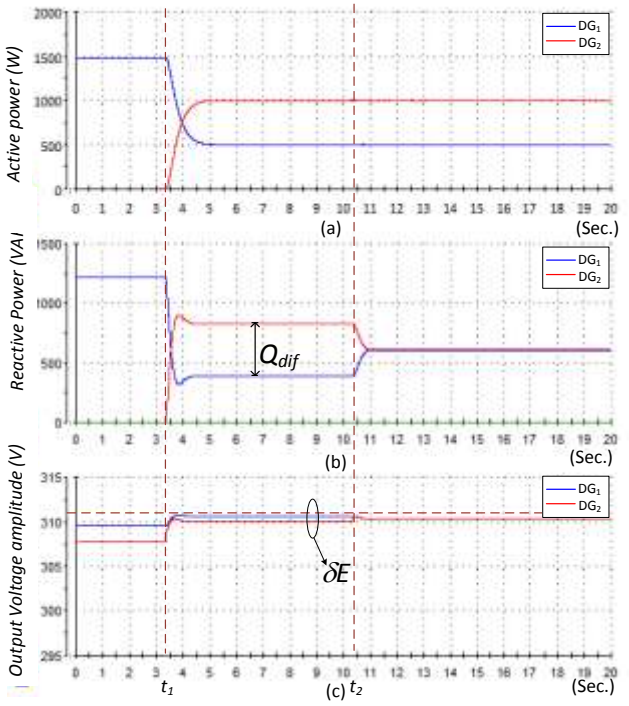

Fig. 11. Active and reactive power distribution with negative virtual impedance.

434Var. At t_2, the droop/reverse droop coefficients increase to n_d=n_r=0.0053, and Q_{dif} decreases to 140Var. It can be seen that increasing droop/reverse droop coefficients can increase

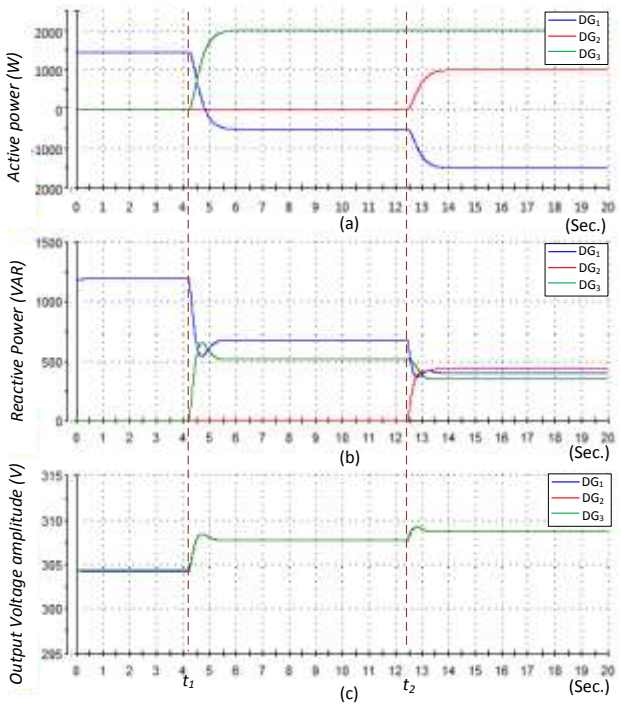

Fig. 12. Active and reactive power distribution with consideration of system capacity.

the reactive power sharing accuracy. But at the same time the bus voltage deviation deteriorates that δE changes from 1V to 4V.

Fig. 11 shows the simulation results of active and reactive power distribution with negative virtual impedance. DG_2 starts up at t_1, and the negative virtual impedance is activated at t_2. It can be seen reactive power difference Q_{dif} is effectively suppressed from 434Var to 15Var without deteriorating the bus voltage deviation. It proves that the reactive power distribution can be more accurate by using virtual impedance compared to the Q_{dif} when the two units sharing equal reactive power.

Fig. 12 shows the simulation results of active and reactive power distribution with consideration of system capacity. In this case, the reactive power of three DG units is distributed adaptively to the active power regulation. DG_3 starts up at t_1, and output active power 2kW, so that DG_1 charges 0.5kW active power. According to (9), Q_{max1}:Q_{max3}=1.32:1, DG_1 should distribute more reactive power than DG_3, so that it can be seen from the results DG_1 and DG_3 provide 673Var and 513Var respectively. Then DG_2 starts up at t_2, and provide 1kW active power to loads. In this scenario, Q_{max1}:Q_{max2}:Q_{max3}=1.16:1.27:1, so that DG_1, DG_2 and DG_3 share the reactive power of loads at 400Var, 440Var and 348Var respectively according to power capacity of each converter at 3kVA, the small difference of reactive power distribution is due to the tolerance of virtual impedance compensation.

VI. CONCLUSION

This paper presented autonomous active and reactive power distribution for integrated CCM and VCM units in islanded microgrids. Based on the droop and reverse droop method, the proper active and reactive power management can be conveniently obtained by assigning primary loop coefficients. The droop and reverse droop control based on the system capacity was proposed so that the reactive power distribution can be adaptively controlled according to active power distribution. And the methods to reduce the reactive power sharing difference were provided. Finally, the Real-time hardware-in-the-loop simulation results were given and verified the proposed control strategy.

REFERENCES

[1] J. M. Guerrero, P. C. Loh, T.-L. Lee, M. Chandorkar, "Advanced Control Architectures for Intelligent Microgrids—Part II: Power Quality, Energy Storage, and AC/DC Microgrids," *IEEE Transactions on Industrial Electronics*, vol. 60, no. 4.

[2] J. M.Guerrero, L. Hang, J. Uceda, "Control of Distributed Uninterruptible Power Supply Systems," *IEEE Transactions on Industrial Electronics*, vol. 55, no. 8, pp. 2845-2859, Aug. 2008.

[3] K. Ilango, A. Bhargav, A. Trivikram, P.S. Kavya, G. Mounika, M.G. Nair, "Power quality improvement using STATCOM with renewable energy sources," *Proc. Power Electronics (IICPE)*, 2012, pp.1,6, 6-8 Dec. 2012.

[4] I. Sefa, N. Altin, S. Ozdemir, "An implementation of grid interactive inverter with reactive power support capability for renewable energy sources," *Proc. Power Engineering, Energy and Electrical Drives (POWERENG)*, pp.1,6, 11-13 May 2011

[5] D. E. Olivares, C. A. Canizares, M. Kazerani, "A centralized optimal energy management system for microgrids," *2011 IEEE Power and Energy Society General Meeting*, pp.1-6, 24-29 July 2011.

[6] A. Tuladhar, H. Jin, T. Unger, K. Mauch, "Control of parallel inverters in distributed AC power systems with consideration of line impedance effect," *IEEE Industry Applications*, vol. 36, no.1, pp.131-138, Jan/Feb 2000.

[7] J. Kim, J. M. Guerrero, P. Rodriguez, R. Teodorescu, N. Kwanghee, "Mode Adaptive Droop Control With Virtual Output Impedances for an Inverter-Based Flexible AC Microgrid," *IEEE Trans. Power Electron.*, vol. 26, no. 3, pp. 689-701, March 2011.

[8] D. Wu, Guerrero, J.M. Guerrero, J. C. Vasquez , T. Dragicevic, F. Tang, "Coordinated power control strategy based on primary-frequency-signaling for islanded microgrids," *Proc. Energy Conversion Congress and Exposition (ECCE)*, pp.1033,1038, 15-19 Sept. 2013

[9] K. T. Tan, P. L. So, Y. C. Chu, and M. Z. Q. Chen, "Coordinated Control and Energy Management of Distributed Generation Inverters in a Microgrid," *IEEE Trans. Power Del.*, vol. 28, pp. 704–713, Apr. 2013.

[10] J.M. Guerrero, J.C. Vasquez, J. Matas, L.G. de Vicuña, M. Castilla, "Hierarchical Control of Droop-Controlled AC and DC Microgrids—A General Approach Toward Standardization," *IEEE Trans. Ind. Electron.*, vol.58, no.1, pp.158,172, Jan. 2011.

[11] J. M. Guerrero, L. GarciadeVicuna, J. Matas, M. Castilla, and J. Miret, "Output Impedance Design of Parallel-Connected UPS Inverters With Wireless Load-Sharing Control," *IEEE Trans. Ind. Electron.*, vol. 52, pp. 1126–1135, Aug. 2005.

[12] J. C. Vasquez, R. A. Mastromauro, J. M. Guerrero, and M. Liserre, "Voltage Support Provided by a Droop-Controlled Multifunctional Inverter," *IEEE Trans. Ind. Electron.*, vol. 56, no. 11, pp. 4510–4519, Nov. 2009.